Bioresource Technology 251 (2018) 249–258

Contents lists available at ScienceDirect

Bioresource Technology

journal homepage: www.elsevier.com/locate/biortech

Life cycle energy and greenhouse gas emission effects of biodiesel in the United States with induced land use change impacts

Rui Chen[a], Zhangcai Qin[a], Jeongwoo Han[a], Michael Wang[a,*], Farzad Taheripour[b], Wallace Tyner[b], Don O'Connor[c], James Duffield[d]

[a] Systems Assessment Group, Energy Systems Division, Argonne National Laboratory, 9700 S. Cass Avenue, Lemont, IL 60439, United States
[b] Department of Agricultural Economics, Purdue University, 403 West State Street, West Lafayette, IN 47907, United States
[c] (S&T)^2 Consultants Inc., 11657 Summit Crescent, Delta, BC V4E 2Z2, Canada
[d] Office of the Chief Economist, United States Department of Agriculture, United States

ARTICLE INFO

Keywords:
Life cycle analysis
Biodiesel
Induced land use change
Fossil energy consumption
Greenhouse gas emissions

ABSTRACT

This study conducted the updated simulations to depict a life cycle analysis (LCA) of the biodiesel production from soybeans and other feedstocks in the U.S. It addressed in details the interaction between LCA and induced land use change (ILUC) for biodiesel. Relative to the conventional petroleum diesel, soy biodiesel could achieve 76% reduction in GHG emissions without considering ILUC, or 66–72% reduction in overall GHG emissions when various ILUC cases were considered. Soy biodiesel's fossil fuel consumption rate was also 80% lower than its petroleum counterpart. Furthermore, this study examined the cause and the implication of each key parameter affecting biodiesel LCA results using a sensitivity analysis, which identified the hot spots for fossil fuel consumption and GHG emissions of biodiesel so that future efforts can be made accordingly. Finally, biodiesel produced from other feedstocks (canola oil and tallow) were also investigated to contrast with soy biodiesel and petroleum diesel.

1. Introduction

While gasoline market in the United States is expected to fall in coming decades due to vehicle efficiency gains and vehicle electrification, annual diesel consumption in transportation will increase from 7.04 to 8.45 quintillion (10^{18}) Joules by 2040 (EIA, 2016a); this is an outcome of the expansion of the freight transportation industry following the continuing economic growth. The opposing trends of these two liquids' future demand could drive many fuel producers to shift their focus from gasoline to diesel. Globally, the consumption of liquid fuels in the transportation sector alone is predicted to grow from 110.3 quintillion Joules in 2015 to 144.3 quintillion Joules in 2040 (EIA, 2016c). The globally expanding demand for transportation fuels has raised serious concerns about supply, energy independence, economic development, environmental stewardship, and human health and wellbeing. Sustainable solutions that address these issues must be explored to meet our future needs. Biomass-based alternative liquid fuels (biofuels) have received heightened interest due to positive attributes such as low life cycle greenhouse gas (GHG) emissions, renewable feedstocks, and their nontoxic and biodegradable residues. In particular, as one of the most commercially produced and consumed biofuels, biodiesel has gained significant popularity worldwide over the past two decades. Of the 5.93 billion liters of biodiesel produced in the United States in 2016, soy oil was the most abundantly used feedstock, accounting for approximately 55% of all reported feedstock inputs, followed by recycled oil/grease (~13%), distillers corn oil (~12%), animal fat (~10%), and other vegetable oils (~10%) (EIA, 2016b). These biodiesel feedstocks can also be categorized into two groups based on their free fatty acids (FFA) content: vegetable oils (such as soy oil and canola oil) that contain low FFA, and high FFA oils (such as corn oil, tallow, and grease). Different levels of FFA in biodiesel feedstocks can significantly impact the amount of energy and chemical inputs during the biodiesel conversion, and a parallel comparison of these two types of oil feedstocks can help understand differences and similarities among feedstocks for biodiesel production.

In general, the life cycle of a specific transportation fuel involves a series of stages that lead from "well" (production of the feedstock) to "wheel" (combustion of the fuel). The GHG emissions from the combustion stage of biofuels are offset by CO_2 fixation while the biomass is growing. However, the production stage of biofuels can generate relatively high GHG emissions due to the use of fossil fuels. Therefore, a life cycle analysis (LCA) of both the environmental flows and the energy

* Corresponding author.
E-mail address: mqwang@anl.gov (M. Wang).

https://doi.org/10.1016/j.biortech.2017.12.031
Received 17 October 2017; Received in revised form 10 December 2017; Accepted 11 December 2017
Available online 15 December 2017

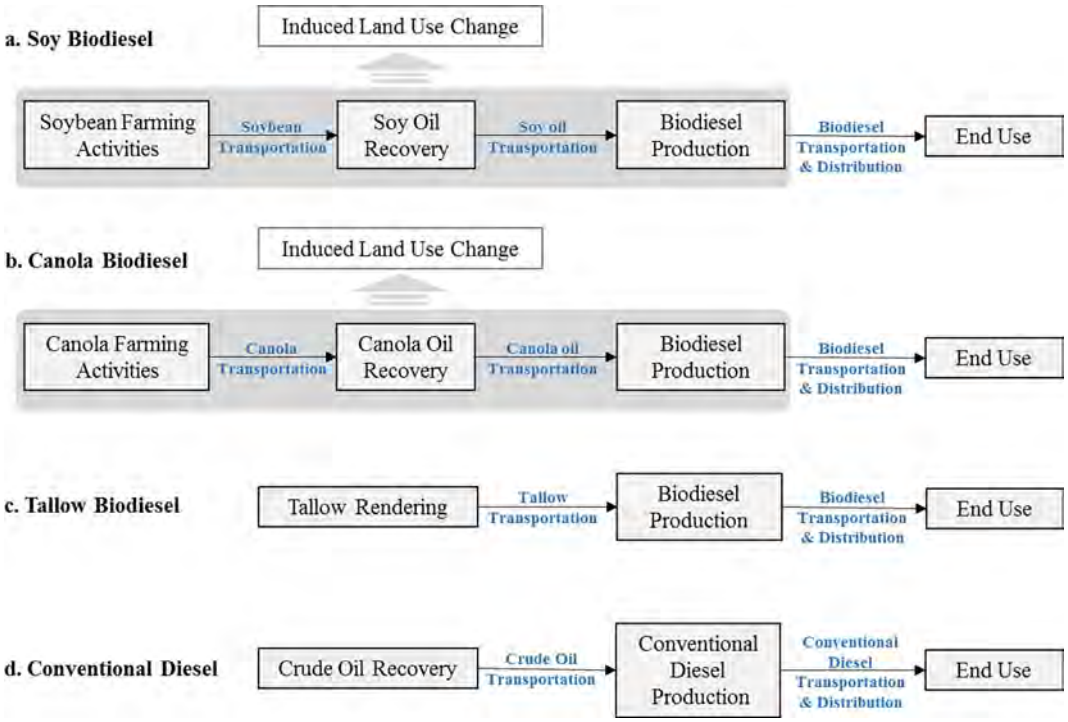

Fig. 1. System boundaries for (a) soy biodiesel, (b) canola biodiesel, (c) tallow biodiesel, and (d) conventional petroleum diesel.

flows of each biofuel is needed to quantify the advantages of biofuel over conventional fossil diesel. Furthermore, timely and representative LCA is also crucial to transportation fuel regulations and directives; it serves as the principle tool with which to evaluate GHG reduction and other environmental impacts from each alternative fuel system (EPA, 2009, CARB, 2016).

A 1998 LCA study by the National Renewable Energy Laboratory (NREL) concluded that pure soybean based biodiesel (B100) and 20% biodiesel blend (B20) used on urban buses could reduce the petroleum fuel consumption by 95% and 19%, respectively, and the CO_2 emissions by 78% and 16%, respectively (Sheehan et al., 1998). Many subsequent LCA studies on biodiesel identified and quantified the areas where further technical improvements can help biodiesel LCA results. Pradhan et al. (2008, 2011, 2012) conducted a series of LCA studies of soy biodiesel, and subsequently concluded that the energy efficiency of biodiesel was increasing over time due to increases in soybean yield and biodiesel conversion efficiency, which indicated that LCA for soy biodiesel should be updated periodically. Several studies used process simulation software to generate the life cycle inventory data (Morais et al., 2010, Milazzo et al., 2013, Varanda et al., 2011), which may introduce another level of uncertainty to the analysis, as well as overlooking many issues such as quality and sources of the feedstock, plant location, product preservation, and nameplate capacity versus actual yield. Additionally, many of these LCA studies lacked of comprehensive assessment of the unintended consequences introduced by biodiesel, such as the induced land use change (ILUC).

In general, the expansion of agricultural production due to the increase in biodiesel demand is considered to cause ILUC and alter carbon balance in the ecosystems specific to land types (e.g., forest, grassland, and cropland). The change in the soil organic carbon (SOC) and nitrous oxide (N_2O) emissions resulting from ILUC will eventually contribute to soy biodiesel's life cycle GHG emissions. Because these effects are difficult to observe or measure directly, they are often simulated using a combination of economic and environmental models. Moreover, different structures among models, as well as various assumptions of key parameters (e.g., location, land type before and after ILUC, ILUC area, ILUC duration, farming practice, and emission factors of land conversion), are usually the main causes of discrepant simulation results (Castanheira and Freire, 2013, Kim and Dale, 2009, Smeets et al., 2009). For instance, the Low Carbon Fuel Standard (LCFS) program by the California Air Resources Board (CARB) reported an indirect land use change GHG emission value for soy biodiesel of 62.0 g CO_2e/MJ in 2009, which was simulated using the first version of the Global Trade Analysis Project (GTAP-BIO) model and emission factors from the Woods Hole Institute (Gohin, 2015). A 2014 revised result using an updated version of GTAP-BIO (Taheripour and Tyner, 2013a) and CARB's AEZ-EF model reduced this emission value to 29.1 g CO_2e/MJ (CARB, 2015, Gohin, 2015). Several improvements in the GTAP-BIO model and its data base contributed to this reduction: 1) updating GTAP database from 2001 to 2004; 2) taking into account yield improvements in crop production between these years; 3) corrections in GTAP database to better represent production of vegetable oils and meals according to actual observations; 4) revisions in modeling animal feeds to take into account substitution among feed crops and oilseeds meals; 5) using updated regional land transformation elasticities according to recent observations; 6) improvements in modeling land extensification in each region by AEZ, and 7) using regional emission factors by AEZ (Taheripour et al., 2017b). Clearly it is important to use up-to-date models and data and to handle the analysis of land use change (Castanheira and Freire, 2013).

In this study, we evaluate the soy biodiesel life cycle GHG emissions and fossil energy consumption by incorporating the most recent survey data on U.S. soybean farming and biodiesel production into the Greenhouse gases, Regulated Emissions, and Energy use in Transportation (GREET®) model developed at Argonne National Laboratory (2016). We also investigate the database and parametric improvements in GTAP-BIO model, and integrate the GTAP-BIO with the Carbon Calculator for Land Use Change from Biofuels Production (CCLUB) module in GREET to assess the soy biodiesel ILUC GHG emissions. For comparison, conventional diesel was used as a baseline. Biodiesel derived from other feedstocks in the U.S., such as canola oil (vegetable oil) and tallow (oil with high free fatty acids content), are also examined to evaluate the impact of feedstock FFA content during the biodiesel conversion

2. Methodology and data sources

The system boundary of the soy biodiesel pathway (Fig. 1a) includes soybean farming activities (i.e., fertilizer and chemical production, soybean cultivation, and harvesting), soybean transportation, soy oil recovery, soy oil transportation, biodiesel production, biodiesel transportation and distribution, biodiesel combustion (including biogenic carbon credit), and ILUC. The ILUC comes from market-mediated responses that can occur worldwide. Essentially, the increased demand for soybeans for biodiesel production results in a soybean price increase, which induces changes in crop switching, consumption of other types of crops, potentially land conversion from forest or pasture to cropland, and other effects. The overall GHG emissions equal to the sum of the GHGs from all components associated to soy biodiesel production within the system boundary, including emissions from the ILUC; this methodology is consistent with previously published studies and LCFS' approach (Wang et al., 2011, Wang et al., 2012, CARB, 2016). The system boundary for the canola biodiesel (Fig. 1b) is similar to soy biodiesel (Cai et al., 2015). Whereas the system boundary for the tallow biodiesel pathway (Fig. 1c) only includes rendering, biodiesel production, and biodiesel combustion, as well as necessary transportation and distribution. With price approximately 20% - 35% of beef prices on a per-tonne basis, tallow has significant economic value. However, for each kilogram of beef meat produced in the United States, about 0.2 kg tallow can be rendered, which makes the production of tallow inelastic with demand. In other words, it is unlikely that farmers would raise cattle mainly for tallow instead of meat. Therefore, tallow is treated as a byproduct from the meat production and does not share burdens from upstream processes such as animal feed production, animal farming, and slaughtering (Han et al., 2014, Lopez et al., 2010).

As shown in Fig. 1d, three key processes in the conventional diesel life cycle are crude oil recovery, petroleum refining, and combustion. Previously reported parameters on the recovery of conventional crude, oil sand, and shale oil were used to estimate the energy intensity and GHG emissions of the crude oil recovery process in this study (Han et al., 2017). The petroleum refining process in this study was based on the analysis of 43 large U.S. refineries in 2012 (Elgowainy et al., 2014). Emissions from the direct land disturbance associated with the oil sand operations are included in the GREET model (Yeh et al., 2014); the indirect impact from the use of conventional diesel (e.g. military operation by the United States to secure its oil access in the Middle East) was relatively small according to previous reports (Wang et al., 2011), and was not considered in this study.

The functional unit of this study is one mega joule (MJ) of the final fuel product (biodiesel or conventional diesel) produced and used.

2.1. Soybean farming

Data for soybean yield and harvested area, as well as nitrogen fertilizer (N), phosphate (P_2O_5), potassium oxide (K_2O), herbicide, and insecticide use in soybean farming were acquired from the National Agricultural Statistics Service by the U.S. Department of Agriculture (USDA-NASS). In particular, the 2015 USDA survey on fertilizer and chemical applications for soybean farming was used in this LCA. Data from the same survey conducted in 2012 were also investigated for comparison. Soybean yield in the United States in 2012 was significantly below historical trends because of drought that year (NOAA-NCEI, 2013). Since soybean yield can influence farming input intensities for the LCA, a 3-year average yield between 2011 and 2013 was used for the calculation of fertilizer, chemicals, and energy consumption in 2012 to account for the abnormal weather impact on farming input intensities. Table 1 summarizes the farming practice and material inputs for 2012 (based on both 1-year and 3-year average yields) and 2015. In comparison, the soybean yield and the harvested area in 2015 increased significantly, while the usage of P_2O_5, K_2O, and insecticides per kg soybeans decreased. This is most likely due to weather conditions, improvements in seed quality, machinery efficiency, and the increased precision of farm management (Schemberger et al., 2017, Specht et al., 1999). The application of fertilizer and chemicals per kg of harvested soybeans was relatively consistent between 2011 and 2013.

Table 1
Yield, harvested area and farming inputs for soybean in the U.S. (all in dry weight).[1]

Surveyed Item	Unit	2012 (1-yr yield)	2012 (3-yr avg. yield)	2015[3]
Yield	kg/hectare	2340	2457	2808
Area harvested	million hectares	31	31	33
N	g/kg soybeans	2.0	2.0	2.0
P_2O_5	g/kg soybeans	8.4	8.3	7.9
K_2O	g/kg soybeans	14.0	13.9	12.6
Herbicides	g/kg soybeans	0.8	0.8	0.8
Insecticides	g/kg soybeans	0.03	0.03	0.02
Diesel[2]	kJ/kg soybeans	610	579	n/a
Gasoline[2]	kJ/kg soybeans	136	129	n/a
LPG[2]	kJ/kg soybeans	34.1	32.4	n/a
Natural Gas	kJ/kg soybeans	43.9	41.6	n/a
Electricity	kJ/kg soybeans	41.7	39.5	n/a

[1] Data source: USDA-NASS for soybean yield, harvested area, fertilizer and chemical inputs; USDA-Economic Research Service (ERS) for soybean farming energy inputs (ARMS tailored report provided by ERS upon request).

[2] The original liquid fuel use in ARMS data is reported by volume. Calculations in this report were based on the low heating value of each fuel.

[3] The most current survey data are used for the simulation in this study: farming yield, area, and material inputs from 2015 and farming energy inputs from 2012.

The most recent data on the direct energy consumption and the fuel sources for field activities (e.g., plantation, cultivation, irrigation, and harvesting) were collected by USDA's ERS ARMS in 2012 (Table 1). The energy usage for soybean drying is included in the ARMS data. Based on this table, the impact of yield on the farming energy input was more obvious than on the fertilizer and chemicals: using the 3-year average yield leads to a total energy consumption of 821.4 MJ/tonne of dry soybeans, which is 5.2% lower than the corresponding value for the 1-year yield for 2012.

2.2. Soy oil recovery

The energy and material inventories for soy oil recovery were obtained from the Omni Tech report (2010), which was based on the National Oilseed Processors Association (NOPA) 2008 survey. In 2014, NOPA updated the electricity use in the soy oil recovery process from previous 289 kWh/tonne of virgin soy oil to 202 kWh/tonne (Zgola et al., 2016). This updated number was incorporated in this study (Table 2). In comparison, a similar study by Pradhan et al. (2011) used

Table 2
Inventory data for soy oil recovery (per kg virgin soy oil).

Material	Unit	per kg virgin soy oil
Input		
Feedstock	kg, dry weight	4.6
Water use/loss	liter	1.16
Total energy:	MJ	7.2
Hexane	MJ	0.13
Electricity	MJ	0.7
Natural gas	MJ	4.1
#2 Fuel oil	MJ	0.03
#6 Fuel oil	MJ	0.06
Coal	MJ	2.0
Biomass energy	MJ	0.06
Landfill gas	MJ	0.03
Output		
Soy oil, virgin	kg	1.0
Soy meal	kg, dry weight	3.5

Table 3
Inventory data for commercial biodiesel transesterification using various feedstocks (per kg biodiesel, all net values).

Material	Unit	Vegetable oil	High-FFA oil
Input (per kg biodiesel)			
Feedstock	kg	1.0	1.1
Sodium methylate	g	4.9	5.2
Sodium hydroxide	g	0.4	0.7
Potassium hydroxide	g	–	0.6
Hydrochloric acid	g	2.5	3.6
Sulfuric acid	g	0.1	0.1
Phosphoric acid	g	0.4	0.3
Citric acid	g	–	0.4
Nitrogen gas	g	2.2	27.5
Methanol	g	108	110
Electricity	kJ	147	311
Natural gas	kJ	1180	2163
Diesel	kJ	–	23.5
Distillation bottoms	kJ	–	13.1
Water withdrawal[1]	liter	0.5	0.9
Output (per kg biodiesel)			
Biodiesel	kg	1.0	1.0
Glycerin[2]	g	90.5	81.5
Fatty acids	g	4.3	77.1
Distillation bottoms	g	3.0	24.3
Water discharge[1]	liter	0.3	0.4

[1] Water withdrawal includes steam water; steam water loss in the cooling tower is assumed to be 1%, the remaining steam water is included in the water discharge. Discharged water is assumed to be recovered onsite.

[2] The FFA content in the original oil feedstock can influence the amount of coproduced glycerin. Because the survey lacks glycerin concentration data, volumes reported in this row reflect an assumed concentration of 80% glycerin.

a process-engineering model to simulate the energy, hexane, and water consumption of the oil recovery process. On the other hand, the European Union's vegetable oil and protein meal industry association (FEDIOL) also published their LCA report of EU oilseed crushing and vegetable oil refining (Schneider and Finkbeiner, 2013); the total energy requirement for soybean crushing in their report was 4.97 MJ/kg virgin soy oil, which included electricity (0.54 MJ/kg virgin soy oil) and fuels (4.42 MJ/kg virgin soy oil, assuming boiler efficiency at 80% and 3.37 MJ energy was required to produce one kilogram of steam). NOPA's total energy input (Table 2) was 43.8% higher than FEDIOL's value, which could be due to NOPA's undefined basis (higher or lower) of heating values and the exclusion or inclusion of plants that purchased steam instead of generating it themselves between NOPA and FEDIOL.

2.3. Biodiesel production through transesterification

Updated inventory data for the commercial biodiesel production process (Table 3) were summarized based on the survey by the National Biodiesel Board (NBB) in 2016. The survey was sent to 64 NBB producing members (9.01 billion liters of total annual biodiesel production capacity, 4.50 billion liters of actual produced volume in 2015), and received 24 responses (4.32 billion liters of total annual biodiesel production capacity, 3.14 billion liters of actual produced volume in 2015). The respondents represented 44% of surveyed NBB plants, 48% of total surveyed capacity, and 70% of surveyed actual production volume in 2015. Among these 24 responses, 12 plants processed vegetable oil (soy and canola oil) exclusively, and 15 plants processed oils (mixed or separately) that contained high FFA (such as corn oil, used cooking oil, and animal fat). In this study, data from the vegetable processing plants were used for the soy and canola biodiesel pathway, whereas data from the high-FFA oil plants were used for the tallow biodiesel pathway.

Compared to the summary of a similar NBB survey from 2008, the updated inventory of soy biodiesel production shows improved biodiesel yield and chemical usage efficiency. One addition to the updated list of input materials is nitrogen gas, which is used as an inert gas to prevent oxidation of the product. The energy requirement also significantly increased in this update, and it correlates with tightened specifications for biodiesel fuel quality and increased adherence to customer demands. In the "Standard Specification for Biodiesel Fuel Blend Stock (B100) for Middle Distillate Fuels (D6751)" by the American Society of Testing and Measurement (ASTM), a number of parameters (e.g., distillation, cloud point, cetane number, monoglyceride) and improved test methods were added over the past few years (ASTM, 2015). These improvements ensure the quality of the product meets consumers' requirements and increased confidence in test results. The U.S. biodiesel quality survey conducted by NREL (Alleman et al., 2013) shows that 95% of the biodiesel (B100) samples (representing 94% of the U.S. market) met ASTM D6751 quality specifications in 2011; in comparison, only 41% of B100 samples from 86 companies met the specification in 2006. NREL's observations also coincide with the strengthened ASTM fuel quality specification in the marketplace.

In the output list, distillation bottoms are heavier methyl ester left after biodiesel separation, which can be used or sold as an energy source; some of the fatty acids can be used for feed and/or industrial application. Hereinafter, the chemical specifications of distillation bottoms and fatty acids are assumed to be the same as residual oil (39.47 MJ/kg energy content, based on low heating value), and the handling method for coproducts was assumed to be the same as for glycerin. As illustrated in Table 3, the biodiesel transesterification process using high-FFA oil is more energy- and chemical-intensive than using vegetable oil of low FFA.

2.4. Coproduct handling methods in LCA

Coproducts can have significant effects on the biodiesel LCA results because they are produced in substantial quantities and possess high potential energy and market values. Process-level hybrid allocation method was applied to all the biodiesel pathways. Briefly, a mass-based allocation between meal and oil was chosen for the oil recovery process, mainly because meals are not an energy product and mass is not subject to market value vacillations (Han et al., 2014). In addition, the biodiesel production (transesterification) process used an energy-based allocation among biodiesel, glycerin, fatty acids, and distillation bottoms to be consistent with CARB LCFS' methodology. For the conventional diesel pathway, we used the process-level energy-based allocation in the GREET model (Elgowainy et al., 2014).

2.5. Induced land use change (ILUC)

The ILUC related GHG emissions were estimated by the CCLUB module in GREET (Dunn et al., 2016). Meanwhile, the AEZ-EF model developed by CARB (Plevin et al., 2014) was used as a reference. Both CCLUB and AEZ-EF estimate emission factors (EFs, in terms of CO_2e per unit of area) for various GHG emissions sources (e.g., biomass loss, and SOC change) and combine the EFs with the GTAP-BIO predicted ILUC to calculate total GHG emissions under each given case. The calculations are generally based on regions defined by GTAP-BIO (i.e., AEZ by 19 regions) for both domestic (within the United States) and international (outside of the United States) ILUC. CCLUB uses a parameterized CENTURY model to simulate spatially specific SOC changes for each ILUC type in the United States (at the county level) (Qin et al., 2016). CCLUB also simulates N_2O emissions related to domestic SOC change at the county level, which enables the model to track GHG emissions at higher spatial resolution so that the estimate can account for local factors such as soil and climate conditions (Dunn et al., 2016).

Four different modeling cases were developed to estimate ILUC for soy biodiesel: CARB Case 8, CARB Average Proxy, GTAP 2004, and GTAP 2011. The first two cases were used by CARB (2015) and they represent a well-established modeling framework that has been

Table 4
Distribution functions of key parameters for the updated biodiesel (BD) pathways.

Parameter	P10	Mean	P90	Distribution function type
Soybean farming				
N fertilizer (g/kg)	0.8	2.0	3.6	Lognormal
P_2O_5 fertilizer (g/kg)	5.0	7.9	12.1	Exponential
K_2O fertilizer (g/kg)	3.5	12.6	23.7	Weibull
Herbicide (g/kg)	0.5	0.8	1.1	Exponential
Insecticide (g/kg)	0.00	0.02	0.04	Lognormal
Total energy (kJ/kg)	290	821	1719	Weibull
Biodiesel production from vegetable oil				
Biodiesel yield (L BD/kg oil)	1.1	1.1	1.2	Logistic
Methanol (kJ/kg BD)	1893	2176	2459	Logistic
Total energy (kJ/kg BD)	809	1349	2138	Exponential
Biodiesel production from high-FFA oil				
Biodiesel yield (L BD/kg oil)	0.9	1.0	1.2	Normal
Methanol (kJ/kg BD)	1624	2209	2795	Logistic
Total energy (kJ/kg BD)	1351	2487	3622	Logistic

developed and improved over time. However, two important deficiencies were identified in the previous version of the GTAP-BIO model as it applied in CARB's previous work. First, the previous version of GTAP-BIO uses an outdated database, which represents the world economy in 2004. Second, this previous version does not include the significant land intensification that has occurred in many regions in recent years across the world due to the expansion in multiple cropping and/or returning idled cropland to crop production (Babcock and Iqbal, 2014). The developers of the GTAP-BIO model recently fixed these two deficiencies (Taheripour et al., 2017a): they updated the database year of this model to 2011 (the latest available GTAP database) and tuned its land use parameters to take into account recent observations in land intensification across the world. The last two cases represent the simulation results based on these updates for soy biodiesel. Details of all four cases are explained below, where YDEL (yield to price response in crop production), PAEL (yield to price response for cropland pasture), and ETA (productivity of new cropland versus existing cropland) are three key parameters for the simulation in GTAP-BIO.

The first simulation case in this study, CARB Case 8, represents one of the 30 cases examined by CARB. This simulation assumes YDEL is 0.25; PAEL is 0.4 in the United States and 0.2 in Brazil; and ETA values are the original estimates developed by Taheripour et al. (2012). These values are close to the default base case values. The second case, CARB Average Proxy, aims to proxy ILUC for the average of the 30 cases developed by CARB. This simulation assumes that YDEL = 0.185 (average of five values selected by CARB); PAEL is 0.3 in the United States (average of PAEL values used by CARB for the United States) and 0.15 in Brazil (average of PAEL values used by CARB for Brazil); and ETA values are the original estimates. The results of the first two cases highlight the role of model parameters in the calculation of ILUC.

The third case, GTAP 2004, uses the 2004 GTAP database but takes into account recent observed intensification in crop production around the world. Compared with the first two cases, this simulation represents the role of intensification in the calculation of ILUC. The last case, GTAP 2011, was based on the updated 2011 GTAP database and takes into account the recent observed intensification in crop production around the world. Compared with case GTAP 2004, the last case highlights the role of the database change in the calculation of ILUC (Taheripour et al., 2017a).

3. Results and discussion

3.1. Fossil energy consumption

GREET was designed with a stochastic simulation tool, which performs various sampling techniques on the input parameters based on their distribution functions in order to address the parametric uncertainties and their impacts on the LCA. The distribution functions of 899 independent parameters are defined in GREET, and the distribution functions of 12 key parameters associated with the biodiesel pathways in this study were defined in Table 4. The lower and upper ends of the error bars in all following figures represent the 10th and 90th percentiles, respectively, of the resulting distributions using Monte Carlo simulations. Final distributions of the GHG emissions and energy consumption result from the variations of the aforementioned parameters for each process (e.g., soybean farming, biodiesel production using various feedstocks). However, due to the lack of statistical data on oil recovery/crushing, energy, and material inputs, these processes did not have distribution functions.

Fig. 2 illustrates the total fossil energy consumption of conventional diesel, soy biodiesel, canola biodiesel, and tallow biodiesel pathways. The baseline conventional diesel pathway requires 1.21 MJ fossil energy for each MJ of diesel consumed. However, the fuel consumption stage for the biodiesel does not contribute to additional fossil fuel depletion due to its renewable feedstocks. The overall fossil energy consumed by the soy biodiesel pathway is 0.239 MJ/MJ, or an 80.1% reduction relative to the conventional diesel. The canola biodiesel pathway in this study results in a fossil energy consumption of 0.317 MJ/MJ. Compared to the soybean pathway, canola is more energy intensive during farming, but less intensive in the oil recovery process.

Unlike the vegetable oil, tallow is derived from beef production, a waste stream from the slaughterhouse, and its fossil energy requirement

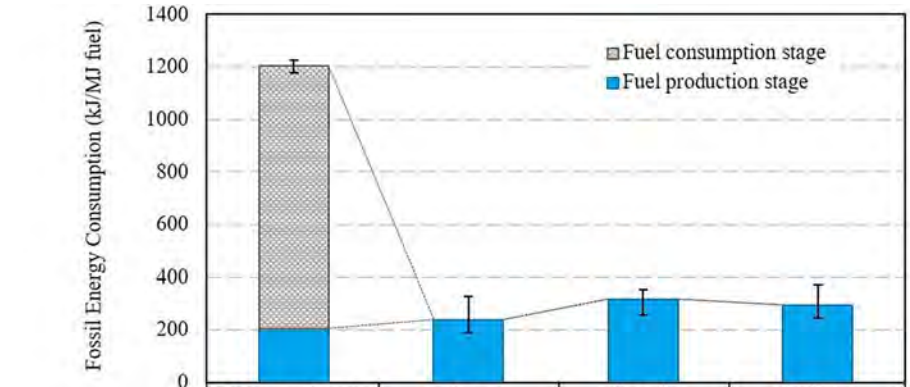

Fig. 2. Overall fossil energy consumption, energy balance and fossil energy ratio (FER) of conventional diesel and biodiesel (B100) from various feedstocks.

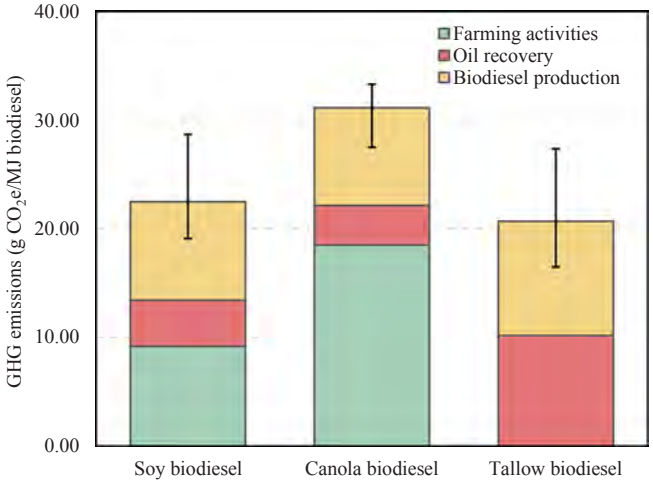

Fig. 3. GHG emissions associated with feedstock-to-biodiesel life cycle (transportation and distribution are included in the processes where intermediates or final fuel are produced).

is 0.294 MJ/MJ. During the fuel production process, the high FFA oil requires either a more intensive reaction condition or an acid-catalyst pretreatment step followed by the alkaline-catalyst transesterification, both of which have higher chemical and energy demands, relative to the vegetable oil conversion (Thanh et al., 2012).

The energy balance and the fossil energy ratio (FER) can also be used to measure the energy intensity for fuel production (Fig. 2). The energy balance represents the difference between the energy content of the final fuel product and the fossil energy consumed during the fuel's life cycle, whereas the FER represents the ratio between the two. All biodiesel fuels from this study have a positive energy balance and an energy ratio above one. Within the fossil energy category, natural gas is in highest demand for all biodiesel pathways. It ranges between 69.3% and 79.3% of the full life cycle fossil energy consumption, followed by petroleum (14.9–19.5%) and coal (5.8%–11.2%).

3.2. Greenhouse gas (GHG) emissions

3.2.1. GHG emissions of feedstock-to-biodiesel production stage

The ensemble of farming activities, oil recovery, biodiesel production, and all necessary transportation/distribution is also referred as the feedstock-to-fuel production stage. Without including the ILUC impact, the GHG emissions from the feedstock-to-fuel production stage (Fig. 3) of soy biodiesel are 22.44 g CO_2e/MJ. Sheehan et al. (1998) compared the GHG emissions of soy biodiesel production to the total petroleum diesel GHG emissions, and concluded that soy biodiesel could achieve a 78.5% reduction of net CO_2 emissions; using the same method, soy biodiesel also reaches a comparable GHG reduction (76.2%) in this study.

The farming process (18.5 g CO_2e/MJ) for canola biodiesel produces significantly higher GHG emissions than that for soybean (9.2 g CO_2e/MJ). This is mostly due to N fertilizer application, given that canola cannot fix N_2 from the atmosphere. The oil recovery process for canola is slightly more efficient than that for soybean because canola has a higher lipid content. This results in a 0.66 g CO_2e/MJ decrease in GHG emissions.

The rendering process of the inedible tallow typically requires it to be cooked at 121 to 135 °C for 1.5 to 2.5 h (Han et al., 2013), which leads to 10.2 g CO_2e/MJ of GHG emissions in the oil recovery process. The transesterification process contributes 10.5 g CO_2e/MJ to the total GHG emissions from tallow biodiesel production; compared to soy biodiesel, this process for high FFA oil has higher GHG emissions because it is more energy and chemical intensive than that for vegetable oil (Fig. 3).

3.2.2. ILUC and associated GHG emissions

Table 5 shows estimated induced land use changes for the examined cases. For CARB Case 8, a soy biodiesel expansion of 3.074 billion liters (0.812 billion U.S. gallons) increases the demand for cropland by 121.9 thousand hectares globally. In this case, only 12.5% of the increase in cropland comes from deforestation and the rest is due to conversion of pasture land. Sub-Saharan Africa and the United States have the largest shares in the new demand for cropland, 40% and 19.2%, respectively. The area of cropland pasture also drops by 269.9 thousand hectares in the United States and by 30.7 thousand hectares in Brazil.

For the CARB Average Proxy case, a soy biodiesel expansion of 3.074 billion liters (0.812 billion U.S. gallons) increases the demand for cropland by 149.2 thousand hectares globally. This average case generates more demand for new cropland than CARB Case 8, due to the changes in the model's YDEL and PAEL parameters. In this case, only 18.2% of the increase in cropland comes from deforestation, and the rest is due to conversion of pasture land. Sub-Saharan Africa and the United States also have the largest shares in the new demand for cropland in this case, 41% and 16.5%, respectively. The area of

Table 5
Induced land use changes for the selected cases and their GHG emissions using two models.

Description		US	EU	Brazil	South America	Malay. & Indon.	Sub-Sah. Africa	Others	World	GHG, AEZ-EF	GHG, CCLUB
		Thousand hectares								g CO_2e/MJ	
CARB Case 8	Forest	−14.5	−1.2	2.2	7.2	−10.8	−8.6	10.5	−15.2	22.4	7.7
	Pasture	−8.9	−2.6	−12.8	−17.3	−1.5	−40.3	−23.2	−106.7		
	Cropland	23.4	3.7	10.6	10.1	12.3	48.8	12.9	121.9		
	Harvested area	23.4	3.7	10.6	10.1	12.3	48.8	12.9	121.9		
	Cropland pasture	−269.9	0.0	−30.7	0.0	0.0	0.0	0.0	−300.6		
CARB Average Proxy	Forest	−16.5	−1.7	−0.4	7.5	−11.3	−14.0	9.1	−27.2	26.1	10.0
	Pasture	−8.2	−3.2	−13.1	−19.2	−1.7	−47.7	−29.1	−122.1		
	Cropland	24.6	4.9	13.4	11.7	13.0	61.6	19.9	149.2		
	Harvested area	24.6	4.9	13.4	11.7	13.0	61.6	20.9	149.2		
	Cropland pasture	−282.7	0.0	−38.1	0.0	0.0	0.0	0.0	−320.8		
GTAP 2004	Forest	−4.3	0.8	1.1	4.4	−8.1	−0.9	4.3	−2.7	16.9	4.3
	Pasture	−0.1	−1.4	−3.3	−12.4	−1.3	−33.5	−7.2	−59.3		
	Cropland	4.5	0.7	2.2	8.1	9.4	34.4	3.0	62.2		
	Harvested area	21.8	3.1	5.3	8.6	9.4	42.3	10.0	100.6		
	Cropland pasture	−271.3	0.0	−30.6	0.0	0.0	0.0	0.0	−301.9		
GTAP 2011	Forest	−0.9	−0.4	−2.0	1.2	−5.9	3.8	0.3	−3.8	18.3	6.3
	Pasture	−1.2	−0.8	−3.3	−5.1	−0.6	−16.4	−4.9	–32.4		
	Cropland	2.0	1.2	5.3	3.9	6.5	12.7	4.6	36.2		
	Harvested area	9.5	5.8	11.6	4.0	6.5	16.3	11.2	64.9		
	Cropland pasture	-42.6	0.0	−18.0	0.0	0.0	0.0	−5.3	−65.8		

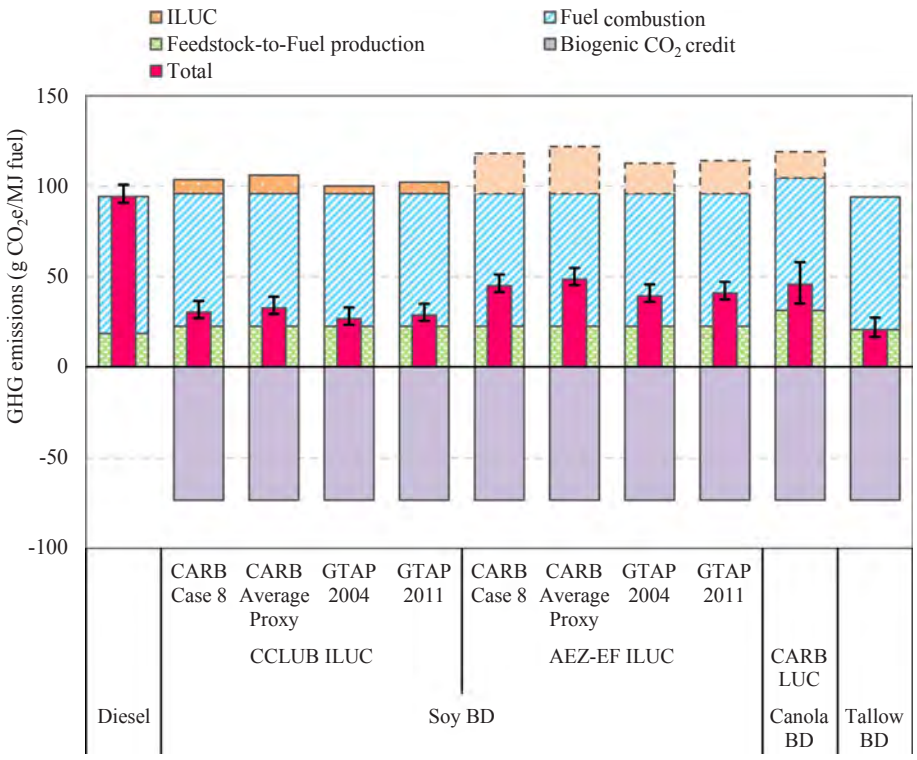

Fig. 4. Overall GHG emissions of conventional diesel and biodiesel (BD) from various feedstocks.

cropland pasture drops by 282.7 thousand hectares in the United States and by 38.1 thousand hectares in Brazil.

In the above two cases (CARB Case 8 and CARB Average Proxy), the changes in harvested area and cropland are identical. This indicates that in these two cases there is no multiple cropping and no use of idled land. Unlike these cases, the next two (GTAP 2004 and GTAP 2011) take into account intensification due to multiple cropping and/or returning unused cropland to crop production. For these two latter cases, changes in harvested areas are larger than the changes in cropland. This indicates that in these cases multiple cropping and/or moving unused cropland to crop production satisfy a portion of the increased demand for cropland.

For GTAP with 2004 data (GTAP 2004), a soy biodiesel expansion of 3.028 billion liters (0.8 billion U.S. gallons) increases demand for cropland by 62.2 thousand hectares globally. In this case, only 4.4% of the increase in cropland comes from deforestation, and the rest is due to conversion of pasture land. Sub-Saharan Africa, Malaysia, Indonesia, and South America have the largest shares in the new demand for cropland.

For GTAP with 2011 data (GTAP 2011), a soy biodiesel expansion of 1.893 billion liters (0.5 billion U.S. gallons) increases demand for cropland by 36.2 thousand hectares globally. In this case, only 10.4% of the increase in cropland comes from deforestation, and the rest is due to conversion of pasture land. Sub-Saharan Africa, Malaysia, Indonesia, and Brazil also have the largest shares in the new demand for cropland.

In terms of the estimated GHG emissions associated with ILUC, cases with cropland intensification (GTAP 2004 and GTAP 2011) generally have lower emissions than the ones without (CARB Case 8 and CARB Average Proxy), regardless of the choice of emission model. The differences among all ILUC cases are largely due to the differences in ILUC type and size predicted by GTAP. In the CARB AEZ-EF model, no emissions are associated with crop switching except for the conversion of cropland pasture to other crops. That may not be true for other emission models. Forest and the pasture normally have much higher carbon stocks, especially SOC stocks, than croplands; consequently, the land use change causes net carbon loss and contributes greater ILUC GHG emissions than the cropland switches.

The ILUC emissions estimated by both emission models share similar trends among various cases. However, AEZ-EF figures are significantly higher than the corresponding CCLUB estimates (Table 5). The differences between ILUC emissions in the two emission models is deeply rooted in various assumptions and parameters. One major discrepancy we observed is the estimation of ILUC emissions related to peatland loss induced by palm production in the Malaysia-Indonesia region. First, forest loss dominates land conversions in this region, and AEZ-EF assumes a significant portion (33%) of the estimated forest loss occurs on peatland (Plevin et al., 2014). However, CCLUB adopts the U.S. Environmental Protection Agency (EPA) methodology, which assesses an average of 5% total land loss (0–44%, varying by administration unit) occurs on peatland (Harris et al., 2009). Second, the conversion of peatland in AEZ-EF results in a loss of 95 Mg CO_2 per hectare per year, about three times as much as the forest-to-cropland conversion in Southeast Asia and over five times higher than the United States. In CCLUB, the emissions from peatland loss in Malaysia and Indonesia are respectively 73 and 75 Mg CO_2 per hectare per year (Harris et al., 2009). These combined differences create significantly higher ILUC emissions in AEZ-EF than in CCLUB (Table 5). As a result, peatland loss contributes 49–74% of the total ILUC emissions in soy biodiesel production using the AEZ-EF model, depending on the modeling case. In contrast, the CCLUB model estimates only 5.2–7.3% of the total ILUC is from the peatland conversion. It becomes apparent that peatland loss can drive ILUC-related GHG emissions in some cases or models. Further efforts are needed to fill the gap between models, as is more up-to-date data. For instance, Koh et al. (2011) reported almost 90% of the palm expansion in Southeast Asia before early 2000 s was on non-peat areas, and only 6% of the peatland (about 880,000 ha) was converted to palm plantations in the same area during that period. In addition, the EPA (2012) reported that only 13% of the palm plantations in Malaysia and 22% in Indonesia were on peat soils in 2009; and the projected incremental palm expansion in 2022 on peatland is 11.5% in the same region. The new observations may serve to improve models estimating ILUC and associated GHG emissions in Southeast Asia.

3.2.3. Total GHG emissions

Fig. 4 illustrates the total GHG emissions of each fuel pathway, which are the sum of the emissions from feedstock-to-fuel production, fuel consumption, the credits from biogenic CO_2 in fuels, and ILUC

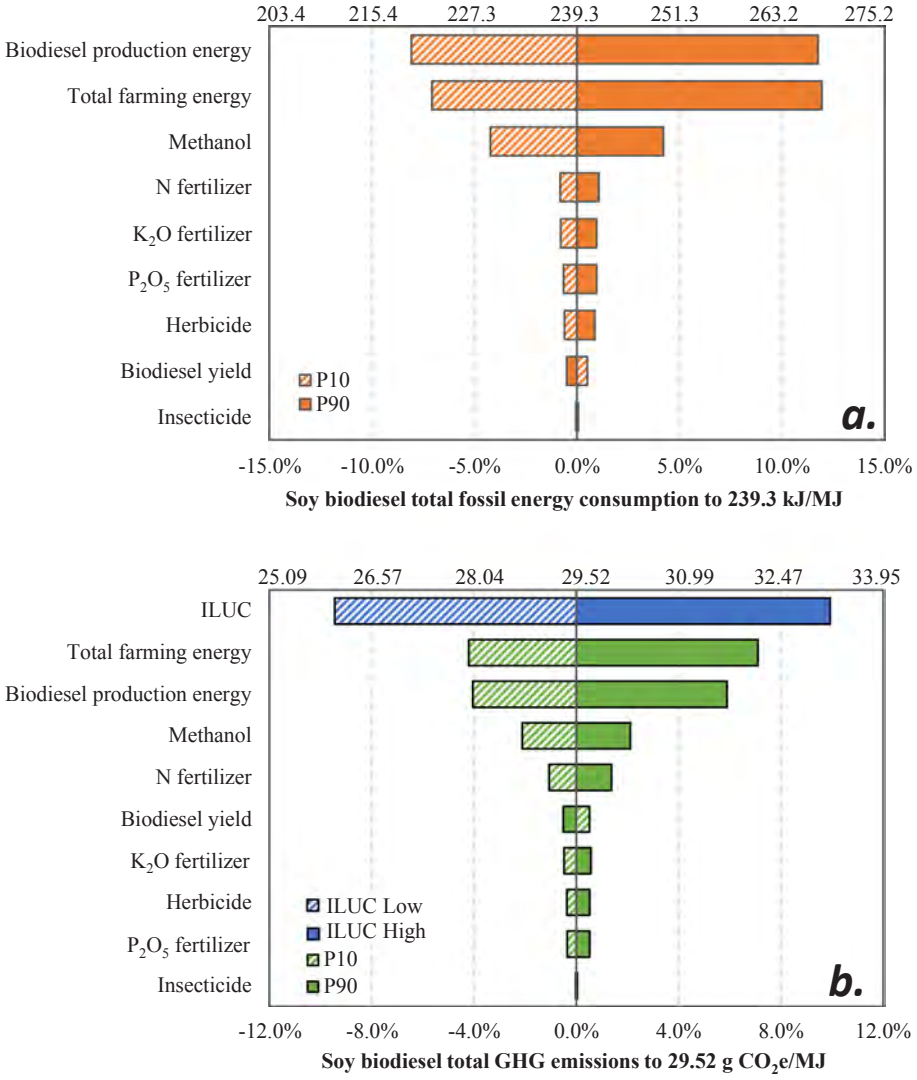

Fig. 5. Sensitivity analyses results for the overall soy biodiesel (a) fossil energy consumption and (b) GHG emissions (average of four ILUC cases with CCLUB).

emissions. Overall, the GHG emissions of baseline conventional diesel are 94.4 g CO_2e/MJ, 80.3% of which is from the end use of diesel. All soy biodiesel ILUC emission scenarios simulated by CCLUB are also presented in this figure: CARB Case 8 contains ILUC parameters that are close to the CARB default base case values, and its total GHG emissions are 30.1 g CO_2e/MJ, which is 68.1% lower than baseline conventional diesel. CARB Average Proxy serves as a proxy for the average of all 30 cases developed by CARB, and its total GHG emissions are 32.4 g CO_2e/MJ. When land intensification is considered, GTAP 2004 case yields 26.7 g CO_2e/MJ of total GHG emissions; taking both the updated database and land intensification into account, the GTAP 2011 case reaches an overall GHG emissions of 28.7 g CO_2e/MJ, a 69.5% reduction relative to diesel. In contrast, all four cases with ILUC emissions modeled by AEZ-EF have higher total GHG emissions, ranging between 39.3 and 48.5 g CO_2e/MJ. However, if one desires to use the indirect land use change emission value provided by CARB (2015), 51.5 g CO_2e/MJ of total emissions would be expected. Detailed discussion regarding ILUC updates can be found in previous section.

Due to the lack of data, this study cites the canola ILUC emission value (14.5 g CO_2e/MJ) from a recent CARB report (2015), resulting in total emissions of 45.6 g CO_2e/MJ, or a reduction of 51.6% relative to the conventional diesel. For tallow biodiesel, no ILUC emission is considered due to its system boundary, and its overall emissions are 20.7 g CO_2e/MJ. Furthermore, although tallow-based biodiesel in this study shows advantages over soy- and canola-based biodiesel from an LCA point of view, tallow feedstock availability will be limited by beef production.

3.3. Sensitivity analyses

We conducted the sensitivity analyses of the soy biodiesel total fossil energy consumption and GHG emissions to present the impact of key parameters identified in Table 4. The 10th (P10) and 90th percentiles (P90) of each parameter were selected as the minimum and maximum values, respectively. For the fossil energy consumption (Fig. 5a), energy inputs from both soybean farming (−7.1% to 11.9% variation from 239.3 kJ/MJ) and biodiesel production (−8.1% to 11.8%) are the most sensitive parameters, followed by methanol consumption (within ± 4.2%) during the transesterification process. Fertilizer (N, P_2O_5, and K_2O) and herbicides have a relatively small impact on the total fossil energy consumption (all within ± 1%). Biodiesel yield is also less sensitive to variations (within ± 0.5%) because of the similarity among transesterification technologies currently used by commercial biodiesel plants. Insecticide is the least sensitive parameter (less than ± 0.1%) in the soy biodiesel pathway, possibly due to its small field application rate as well as the utilization of genetically engineered crop seeds.

Fig. 5b illustrates the sensitivity results of the total GHG emissions from the soy biodiesel pathway. ILUC uncertainties can stem from simulations of both ILUC and ILUC emission factors (Taheripour and Tyner, 2013b). The former is affected by GTAP assumptions and

parameterization (Taheripour et al., 2017a), the latter can be modeled spatially explicit for various land management (Qin et al., 2016, Qin et al., 2015). To simplify the simulation, the aforementioned four cases (Table 5) were used to test the sensitivity associated with ILUC, by using averaged CCLUB ILUC emissions of these four cases as the ILUC impact with the highest and the lowest CCLUB ILUC values of the four cases being the boundary. Results indicate ILUC is the most sensitive parameter to the overall GHG emissions (-9.9% to 10.4% variation from 29.6 g CO_{2e}/MJ), followed by the energy inputs in soybean farming (−4.4%–7.5%) and in biodiesel production (−4.2% to 6.2%). The N fertilizer usually has significant impact on the GHG emissions from the farming stage for crops such as corn, sugarcane, switchgrass, and *Miscanthus* (Wang et al., 2012). However, N fertilizer is less sensitive to fluctuations (−1.1% to 1.5%) for soybean because the plants are able to fix atmospheric nitrogen gas to ammonia through their symbiotic relationship with a collection of soil bacteria called “rhizobia”. Some previous studies even suggested forgoing the application of N fertilizer during soybean production because N_2-fixation and soybean plant residues in soil should supply sufficient nitrogen in no-tillage and reduced-tillage soybean farms (Cavalett and Ortega, 2010). Other fertilizer and chemicals (P_2O_5, K_2O, herbicides, and pesticides) as well as biodiesel yield also show low sensitivity (all within −0.4% to 0.6%) to the total GHG emissions. The soy oil recovery process was not considered in the sensitivity analysis due to a lack of data.

It is worth noting that the European Commission and several other international regulatory bodies adopted energy-based allocation for all their pathways; using their methodology, the fossil energy consumption of soy biodiesel could reach 333.9 kJ/MJ; the total GHG emissions would be between 39.6 and 45.3 g CO_{2e}/MJ, depending on the choice of ILUC case. These values are significantly higher than the ones derived from the hybrid allocation method used in this study, mainly due to the large amount of soy meal produced (76.1% dry weight of the soybean) and soy meal’s relatively low energy content (13.15 MJ/kg soy meal vs. 37.20 MJ/kg soy oil).

Many previous studies had established the framework of the soy biodiesel LCA and documented the simulation methodologies using various models. However, given the nature of LCA as well as its potential impact on the environmental and energy policies, emerging issues due to the evolving technologies and data quality must be addressed. Even though both GREET and GTAP models have significant global impacts as they provide useful tools and data on the environmental and economic issues of biofuels, this study not only provided the updated parameters in both models; it also addressed the gap between the direct (core LCA) and the indirect (induced land use change) effects of the soy biodiesel in the U.S. In addition, it examined the cause and the implication of each key parameter via sensitivity analyses, which identified the hot spots for GHG emissions and energy use so that further research and development efforts can be allocated accordingly.

4. Conclusion

This study incorporated most up-to-date survey results and refined modeling tools to demonstrate an extensive life cycle analysis (LCA) of soy biodiesel in the U.S. It combined the process-based LCA and impacts from the ILUC to address the gap between the two in previously published literatures. Our results showed that soy biodiesel could achieve 80% reduction in fossil energy consumption and 66–72% reduction in overall GHG emissions, relative to its petroleum counterpart. A sensitivity analysis also identified that ILUC and energy inputs are the soy biodiesel life cycle hot spots, which should be the focal points of future efforts.

Acknowledgements

The research effort by Argonne National Laboratory was supported by the Bioenergy Technologies Office and the Clean Cities Program of the U.S. Department of Energy (Contract DE-AC02-06CH11357), as well as the Office of Energy Policy and New Uses of the U.S. Department of Agriculture. The effort by Purdue University was supported by the National Biodiesel Foundation. The survey of life cycle inventory data from U.S. biodiesel producers was coordinated by Mr. Don Scott of the National Biodiesel Board and Mr. Don O’Connor; their effort was supported by the Nebraska Soybean Board. We would also like to thank Dr. Harry Baumes of the USDA Office of Energy Policy and New Uses and Dr. Hao Cui of Purdue University for helpful comments on the study.

References

Alleman, T.L., Fouts, L., Chupka, G., 2013. Quality Parameters and Chemical Analysis for Biodiesel Produced in the United States in 2011. National Renewable Energy Laboratory (NREL/TP-5400-57662), Golden, CO.

ASTM, 2015. Standard Specification for Biodiesel Fuel Blend Stock (B100) for Middle Distillate Fuels. West Conshohocken, PA, 2015 (D6751-15ce1).

Argonne National Laboratory, 2016. Greenhouse Gases, Regulated Emissions, and Energy Use in Transportation (GREET) Model. https://greet.es.anl.gov/index.php (accessed 18.05.17).

Babcock, B.A., Iqbal, Z., 2014. Using Recent Land Use Changes to Validate Land Use Change Models. Iowa State University, Ames, IA (14-SR 109).

Cai, H., Han, J., Elgowainy, A., Wang, M., 2015. Parameters of Canola Biofuel Production Pathways in GREET. Argonne National Laboratory. https://greet.es.anl.gov/publication-canadian-canola (accessed 05.18.17).

CARB, 2015. Staff Report: Calculating Carbon Intensity Values from Indirect Land Use Change of Crop-Based Biofuels, Sacramento, CA: California Environmental Protection Agency-Air Resources Board https://www.arb.ca.gov/fuels/lcfs/iluc_assessment/iluc_assessment.htm 2015 (accessed 18.05.17).

CARB, 2016. Low Carbon Fuel Standard: LCFS Basics: California Environmental Protection Agency Air Resources Board. https://www.arb.ca.gov/fuels/lcfs/background/basics.htm (accessed 18.05.17).

Castanheira, E.G., Freire, F., 2013. Greenhouse gas assessment of soybean production: implications of land use change and different cultivation systems. J. Clean. Prod. 54, 49–60.

Cavalett, O., Ortega, E., 2010. Integrated environmental assessment of biodiesel production from soybean in Brazil. J. Clean. Prod. 18 (1), 55–70.

Dunn, J.B., Qin, Z., Mueller, S., Kwon, H.-Y., Wander, M.M., Wang, M., 2016. Carbon Calculator for Land Use Change from Biofuels Production (CCLUB): Users’ Manual and Technical Documentation. Argonne National Laboratory (ANL/ESD/12-5, Rev. 3). https://greet.es.anl.gov/publication-cclub-manual (accessed: 18.05.17).

EIA, 2016a. Annual Energy Outlook 2016 (DOE/EIA-0383). http://www.eia.gov/forecasts/aeo (accessed: 18.05.17).

EIA, 2016b. Biodiesel production capacity and production. http://www.eia.gov/biofuels/biodiesel/production/ (accessed 18.05.17).

EIA, 2016c. International Energy Outlook 2016, With Projections to 2040 (DOE/EIA-0484). http://www.eia.gov/forecasts/ieo (Accessed: 5/18/2017).

Elgowainy, A., Han, J., Cai, H., Wang, M., Forman, G.S., DiVita, V.B., 2014. Energy efficiency and greenhouse gas emission intensity of petroleum products at US refineries. Environ. Sci. Technol. 48 (13), 7612–7624.

EPA, 2009. EPA Proposes New Regulations for the National Renewable Fuel Standard Program for 2010 and Beyond (EPA-420-F-09-023).

EPA, 2012. Notice of Data Availability Concerning Renewable Fuels Produced from Palm Oil Under the RFS Program, 77 FR 4300 (EPA-HQ-OAR-2011-0542FRL-9608-8).

Gohin, A., 2015. Understanding the revised land use changes and greenhouse gas emissions induced by biofuels. Working Paper SMART-LERECO No. 15-08. http://www.ethanolrfa.org/wp-content/uploads/2015/09/b2864d98c6dc508f49_u5m6bhvg0.pdf (accessed: 30.05.17).

Han, J., Elgowainy, A., Cai, H., Wang, M., 2014. Update to Soybean c in GREET: Argonne National Laboratory. https://greet.es.anl.gov/publication-soybean-biodiesel-2014 (accessed 18.05.17).

Han, J., Elgowainy, A., Wang, M., 2013. Development of Tallow-based Biodiesel Pathway in GREET: Argonne National Laboratory. https://greet.es.anl.gov/publication-tallow-13 (accessed: 18.05.17).

Han, J., Tao, L., Wang, M., 2017. Well-to-wake analysis of ethanol-to-jet and sugar-to-jet pathways. Biotechnol. Biofuels 10 (21). http://dx.doi.org/10.1186/s13068-017-0698-z.

Harris, N., Grimland, S. Brown, S., 2009. Land use change and emission factors: updates since the RFS proposed rule: Winrock International. Docket ID: EPA-HQ-OAR-2005-0161-3163). https://www.regulations.gov/document?D=EPA-HQ-OAR-2005-0161-3163 (accessed 18.05.17).

Kim, S., Dale, B.E., 2009. Regional variations in greenhouse gas emissions of biobased products in the United States-corn-based ethanol and soybean oil. Int. J. Life Cycle Assess. 14 (6), 540–546.

Koh, L.P., Miettinen, J., Liew, S.C., Ghazoul, J., 2011. Remotely sensed evidence of tropical peatland conversion to oil palm. Proc. Natl. Acad. Sci. U.S.A. 108 (12), 5127–5132.

Lopez, D.E., Mullins, J.C., Bruce, D.A., 2010. Energy life cycle assessment for the production of biodiesel from rendered lipids in the United States. Ind. Eng. Chem. Res. 49 (5), 2419–2432.

Milazzo, M.F., Spina, F., Primerano, P., Bart, J.C.J., 2013. Soy biodiesel pathways: Global prospects. Renewable Sustainable Energy Rev. 26, 579–624.

Morais, S., Mata, T.M., Martins, A.A., Pinto, G.A., Costa, C.A.V., 2010. Simulation and life cycle assessment of process design alternatives for biodiesel production from waste vegetable oils. J. Clean Prod. 18 (13), 1251–1259.

NOAA-NCEI, 2013. State of the Climate: National Climate Report for Annual 2012. National Oceanic and Atmospheric Administration-National Centers for Environmental Information. https://www.ncdc.noaa.gov/sotc/national/201213 (accessed 18.05.17).

Omni Tech International, 2010. Life Cycle Impact of Soybean Production and Soy Industrial Products: The United Soybean Board. http://biodiesel.org/reports/20100201_gen-422.pdf (accessed 18.05.17).

Plevin, R.J., Gibbs, H.K., Duffy, J., Yui, S., Yeh, S., 2014. Agro-ecological Zone Emission Factor (AEZ-EF) Model. https://www.arb.ca.gov/fuels/lcfs/lcfs_meetings/aezef-report.pdf (accessed 18.05.17).

Pradhan, A., Shrestha, D.S., McAloon, A., Yee, W., Haas, M., Duffield, J.A., 2011. Energy life-cycle assessment of soybean biodiesel revisited. Trans. ASABE 54 (3), 1031–1039.

Pradhan, A., Shrestha, D.S., Van Gerpen, J., Duffield, J., 2008. The energy balance of soybean oil biodiesel production: a review of past studies. Trans. ASABE 51 (1), 185–194.

Pradhan, A., Shrestha, D.S., Van Gerpen, J., McAloon, A., Yee, W., Haas, M., Duffield, J.A., 2012. Reassessment of life cycle greenhouse gas emissions for soybean biodiesel. Trans. ASABE 55 (6), 2257–2264.

Qin, Z., Canter, C.E., Dunn, J.B., Mueller, S., Kwon, H., Han, J., Wander, M., Wang, M., 2015. Incorporating Agricultural Management Practices into the Assessment of Soil Carbon Change and Life-Cycle Greenhouse Gas Emissions of Corn Stover Ethanol Production. Argonne National Laboratory (ANL/ESD-15/26). https://greet.es.anl.gov/publication-cclub-land-management (accessed 18.05.17).

Qin, Z.C., Dunn, J.B., Kwon, H., Mueller, S., Wander, M.M., 2016. Influence of spatially dependent, modeled soil carbon emission factors on life-cycle greenhouse gas emissions of corn and cellulosic ethanol. Glob. Change Biol. Bioenergy 8 (6), 1136–1149.

Schemberger, E.E., Fontana, F.S., Johann, J.A., de Souza, E.G., 2017. Data mining for the assessment of management areas in precision agriculture. J. Eng. Agric. 37 (1), 185–193.

Schneider, L., Finkbeiner, M., 2013. Life Cycle Assessment of EU Oilseed Crushing and Vegetable Oil Refining: Sustainable Engineering. http://www.fediol.eu/data/Full%20FEDIOL%20LCA%20report_05062013_CR%20statement.pdf (accessed 18.05.17).

Sheehan, J., Camobreco, V., Duffield, J., Graboski, M., Shapouri, H., 1998. A overview of biodiesel and petroleum diesel life cycles. National Renewable Energy Laboratory (NREL/TP-580-24772).

Smeets, E.M.W., Bouwmanw, L.F., Stehfest, E., van Vuuren, D.P., Posthuma, A., 2009. Contribution of N_2O to the greenhouse gas balance of first-generation biofuels. Glob. Change Biol. 15 (1), 1–23.

Specht, J.E., Hume, D.J., Kumudini, S.V., 1999. Soybean yield potential – a genetic and physiological perspective. Crop Sci. 39 (6), 1560–1570.

Taheripour, F., Cui, H., Tyner, W.E., 2017a. An exploration of agricultural land use change at the intensive and extensive margins: implications for biofuels induced land use change modeling. In: Qin, Z., Mishra, U., Hastings, A. (Eds.), Bioenergy and Land Use Change. American Geophysical Union (Wiley), Hoboken, NJ.

Taheripour, F., Tyner, W.E., 2013a. Biofuels and land use change: applying recent evidence to model estimates. App. Sci. (Basel) 3 (1), 14–38.

Taheripour, F., Tyner, W.E., 2013b. Induced land use emissions due to first and second generation biofuels and uncertainty in land use emissions factors. Res. Int. Econ. http://dx.doi.org/10.1155/2013/315787.

Taheripour, F., Zhao, X., Tyner, W.E., 2017b. The impact of considering land intensification and updated data on biofuels land use change and emissions estimates. Biotechnol. Biofuels 10, 191.

Taheripour, F., Zhuang, Q., Tyner, W.E., Lu, X., 2012. Biofuels, cropland expansion, and the extensive margin. Energy Sustainable Soc. 2 (25), 11.

Thanh, L.T., Okitsu, K., Boi, L.V., Maeda, Y., 2012. Catalytic technologies for biodiesel fuel production and utilization of glycerol: a review. Catalysts 2 (1), 191–222.

Varanda, M.G., Pinto, G., Martins, F., 2011. Life cycle analysis of biodiesel production. Fuel Process. Technol. 92 (5), 1087–1094.

Wang, M., Han, J., Dunn, J.B., Cai, H., Elgowainy, A., 2012. Well-to-wheels energy use and greenhouse gas emissions of ethanol from corn, sugarcane and cellulosic biomass for US use. Environ. Res. Lett. 7 (4).

Wang, M.Q., Han, J., Haq, Z., Tyner, W.E., Wu, M., Elgowainy, A., 2011. Energy and greenhouse gas emission effects of corn and cellulosic ethanol with technology improvements and land use changes. Biomass Bioenergy. 35 (5), 1885–1896.

Yeh, S., Zhao, A., Hogan, S., 2014. Spatial and Temporal Analysis of Land Use Disturbance and Greenhouse Gas Emissions from Canadian Oil Sands Production. Institute of Transportation Studies, University of California, Davis. https://greet.es.anl.gov/publication-luc-canadian-os (accessed 18.05.17).

Zgola, M., Reinhard, J., Liao, X., Simonnin, G., Gmuender, S., Dettling, J., Benoit Norris, C., Parent, J., Couture, J.-M., 2016. Update of Soybean Life Cycle Analysis: Quantis-New Earth-AGECO. https://unitedsoybean.org/wp-content/uploads/Quantis_USB_SoybeanLCA_FinalReport_trunc_20160825.pdf (accessed 18.05.17).